Cooperative Area Coverage

Liam Paull, Mae Seto, and John J. Leonard

I. Introduction

The area coverage problem is an ideal candidate for multi-robot systems since it is inherently parallelizable. In a naive implementation, a team of N robots should be able to cover an area A roughly N times faster if the area to be covered can be easily decomposed into sub-areas of size A/N.

One often-overlooked issue in the context of area coverage planning is the uncertainty of the sensor platform. In some cases this can be neglected, but in many cases it can not. In the case that platform uncertainty is significant, if the agents can communicate and make relative measurements of each other, then they can improve their respective trajectory estimates. This results is further potential benefits for the multi-robot approach to area coverage.

This work propose a framework for cooperative area coverage within a multi-robot system that is: 1) robust to robot platform uncertainty, 2) applicable to severely unreliable and bandwidth constrained communication links. The result is the first known work that considers robotic area coverage planning, cooperative state estimation, and communication through a possibly constrained channel as one coupled and fully integrated system, as shown in Fig. 1.

A. Autonomous Underwater Minehunting as an Area Coverage Problem

We specifically consider the underwater minehunting scenario as a safety-critical motivating example of the generally applicable principles. In this case, a team of AUVs is deployed to scan an area of seabed with sideways looking sonars. As a vehicle traverses in rectilinear motion, the returns from the sonar are compiled and mosaicked into an image of the seabed which is later examined for possible mine-like objects (MLOs) (See Fig. 2). Recently, some effort has been made to characterize the performance of these mine-hunting sonars [1], which is highly dependent on environmental conditions, altitude of the platform, seabed type, and other factors. For example, the models, or $P(y)$ curves, for three sample seabed types are shown in Fig. 2 - bottom, where the horizontal axis is the lateral distance from the vehicle track, and the vertical axis is the "confidence" or probability of correctly detecting a mine if one exists.

This model presupposes that the location of the vehicle, which defines the '0' point on the horizontal axis, is accurately known. Typically, a vehicle will obtain a GPS fix at the surface and then submerge and propagate its position estimate through a combination of Doppler and inertial sensors (for a full overview of AUV localization and navigation methods see the recent review [2]). As a result, the vehicle estimate will drift while it is submerged. Consider Fig. 3 where more "covered" (higher confidence) areas are more red and less covered areas are blue. In this case, there is a drastic discrepancy between the *desired*, *estimated*, and *actual* area coverage obtained, which is unacceptable for decision-makers who are trying to evaluate the risk of moving personnel or other high-valued assets through the area.

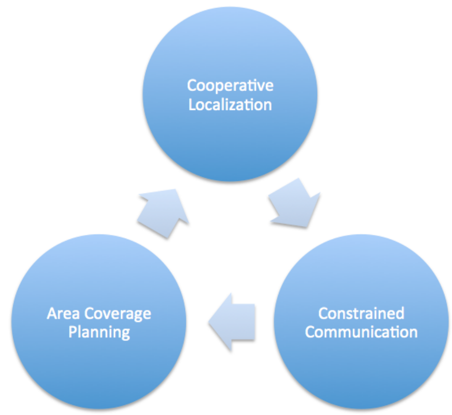

Fig. 1. In the proposed approach area coverage planning, cooperative estimation, and communication through a constrained channel are all considered as one coupled and integrated system.

The literature is extremely scarce with respect to coverage algorithms that even acknowledge the fact that platform location estimation is probabilistic (examples of publications where vehicle uncertainty is mentioned in passing include [3], [4]). Perhaps most related is the 'probably approximately correct' formulation for stochastic coverage defined by Das et al. [5]. This measure defines the probability of coverage of a given fraction of the workspace based on the platform pose uncertainty. However, this approach assumes that platform localization error is constant. In this work, we explicitly connect the sensor platform uncertainty with the coverage uncertainty by mapping the coverage sensor pose posterior through the coverage sensor function (in this case the $P(y)$ curve).

B. Underwater Cooperative Localization

Underwater, communications over any appreciable distance is restricted to the acoustic channel, which is challenging due to its high latency (signals travel at speed of

This work was partially supported by Office of Naval Research (ONR) under grant no. N00014-13-1-0588, NSF Award IIS-1318392, and ONR Global.

L. Paull and J. Leonard are with the Computer Science and Artificial Intelligence Laboratory (CSAIL), MIT, Cambridge, MA 02139, USA. Email: {lpaull,jleonard}@mit.edu

M. Seto is with the Defense R&D Canada, Dartmouth, Nova Scotia, Canada. Email: mae.seto@drdc-rddc.gc.ca

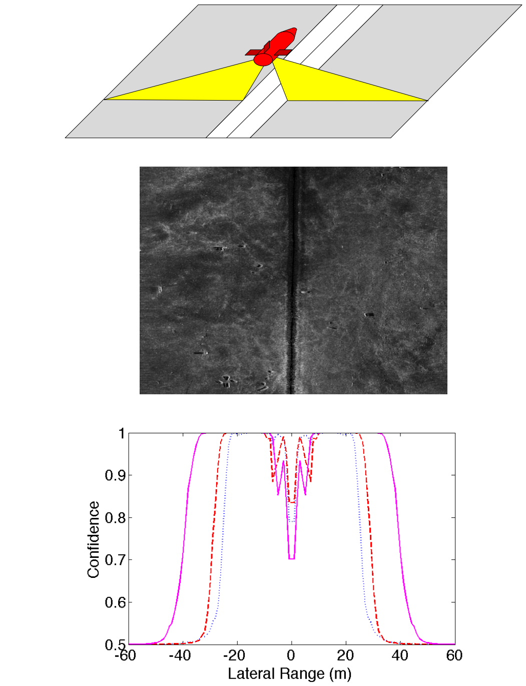

Fig. 2. **Sidescan sonar for area coverage**. *Top*: The sidescan sonar operates by emitting sonar pings in the direction orthogonal to the direction of AUV motion and measuring the time-of-flight of the returns. *Middle*: The resulting data are compiled into a single high-resolution image of the seabed which is used to search for mine-like objects. *Bottom*: The performance of the sidescan sonar for finding mines is highly dependent on many environmental factors. Here, we show three sample models, called $P(y)$ curves, for three different seabed types.

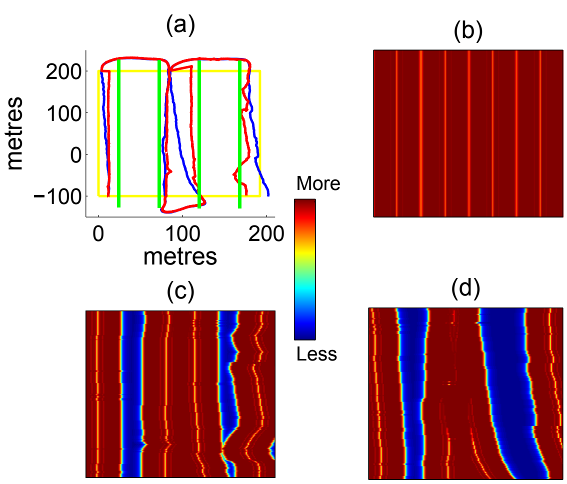

Fig. 3. **(a)** Plot of environment to be covered (yellow) with desired tracks (green), estimated path (red), and actual path (blue). **(b)** Desired coverage. **(c)** Estimated coverage from output of an extended Kalman filter. **(d)** Actual coverage based on ground truth position data.

sound $\approx$ 1500m/s), reduced throughput ($\approx$ 10-100 bytes/s), reduced bandwidth (channel sharing with time division multiple access) and low reliability ($\approx$ 20-50% dropout rate).

Although many works on terrestrial cooperative localization with communication constraints [6]–[8] cite the underwater case as a potential application, they all make assumptions that violate the true nature of the acoustic channel.

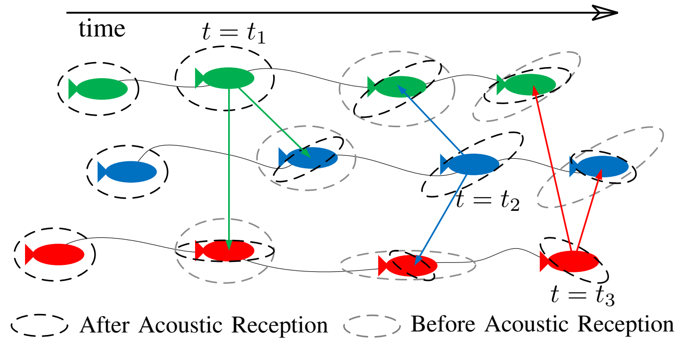

Fig. 4. Conceptual figure showing acoustic communications amongst three AUVs in a time division multiple access scheme. Green AUV transmits at time t_1, followed by the blue one at time t_2, and finally the red one at time t_3. Each reception enables the receiver to obtain a relative range measurement of the sender based on the travel time of the packet and reduce its location uncertainty in the direction of the sender (gray ellipse to black ellipse).

A conceptualization of underwater cooperative localization based on acoustics is shown in Fig. 4. Each vehicle takes a turn broadcasting an acoustic transmission. Any vehicle that makes a reception can also make a range measurement relative to the sender by calculating the time-of-flight of the packet and using precisely synchronized onboard clocks. Several other works [9]–[13] have used a similar setup for underwater cooperative localization. Here, we propose a *smoothing-based* and *non-hierarchical* approach and *apply* it to the task of distributed area coverage.

II. Proposed Approach

In overview, the approach has the following components:

1) We use a probabilistic framework to model the area coverage problem. Within this framework we explicitly link the uncertainty of the robotic platform to the ability to perform area coverage.
2) We present a cooperative trajectory estimation scheme that is permissible in the severely bandwidth-constrained acoustic communications case. This method is particularly well-suited to the area coverage application since area covered is a function of the entire vehicle trajectory, rather than the instantaneous (filtered) estimate.
3) We propose a feedback control scheme that can incorporate the most up-to-date trajectory estimates and dynamically exploit the reduction in trajectory covariance that results from an acoustic packet reception and range measurement.

A. Probabilistic Area Coverage

Here we summarize our approach to accounting for vehicle uncertainty which is presented in more detail in [14]. The workspace to be covered is discretized into cells whose size is commensurate with the resolution of the sensor/actuator being used for area coverage. A random variable W_t^i is

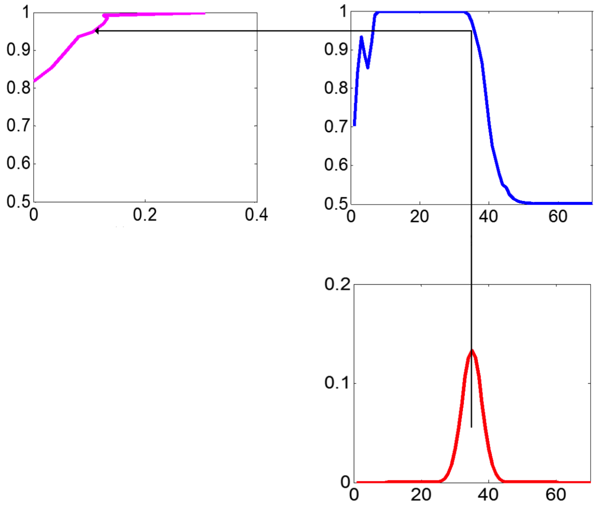

Fig. 5. The distribution of the cell in the sensor frame (bottom right) is mapped through the $P(y)$ curve (top right) to obtain a coverage distribution (top left).

initialized for each cell. The distribution $p(W_t^i = w)$ is estimated through an iterative process consisting of the following steps at each time t for each cell c^i in the sensor swath:

1) Project c^i into the uncertain sensor frame.
2) Estimate the resulting coverage by projecting the uncertain cell location through the coverage sensor function (in this case the $\mathcal{P}(y)$ function shown in Fig. 2 - bottom) as shown in Fig. 5.
3) Combine the coverage with previous "covers" of the corresponding cell through application of the probabilistic MAX function.

The result is a recursive probabilistic coverage estimation framework that scales constantly with time and the size of the workspace to be covered. The probabilistic coverage map is used in combination with some user-specified metric for complete coverage by the adaptive planner described in Sec. II-C.

B. Communication Constrained Cooperative Trajectory Estimation

The approach to cooperative trajectory estimation is similar to the approach we previously proposed in [15]. We employ a graph-based approach and leverage recent results in efficient iterative graphical SLAM solvers (e.g. [16]) to formulate the full multi-vehicle trajectory optimization problem. However, to meet the requirements of the acoustic communications channel, we remove all poses between measurement/communication times as shown in Fig. 6. In addition, a bookkeeping method is used to ensure that all local decentralized graphs remain connected and consistent. The result is a real-time decentralized cooperative trajectory scheme where each vehicle estimates their own trajectory at a dense time resolution (e.g. 4Hz) and the poses of other vehicles only at communication/relative measurement times.

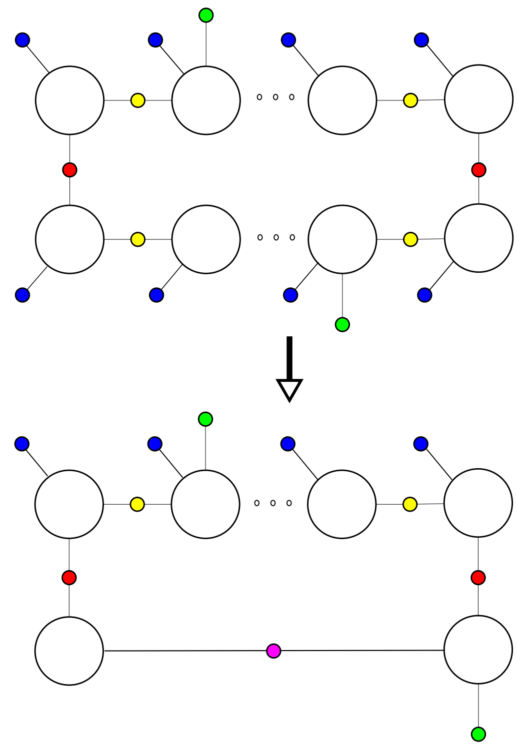

Fig. 6. **Decentralized cooperative trajectory estimation** *top*: Centralized factor graph with compass (blue), GPS (green), DVL-derived odometry (yellow), and relative range (red) factors. *bottom*: intermediate poses between communication/measurement times are removed and replaced with one combined factor (purple).

C. Uncertainty-Aware Adaptive Coverage Planning

We propose a feedback tracking controller to track the value of d shown in Fig. 7. The value of d is calculated to maximize coverage while guaranteeing complete coverage in the survey direction, as indicated in the figure. When vehicle position uncertainty is high, the tracks will need to be spaced more closely in order to guarantee coverage, which is potentially inefficient. Upon reception of an acoustic packet, the entire vehicle trajectory is updated with reduced uncertainty, and consequently the value of d, which corresponds to the spacing of the current track, can be increased resulting in faster coverage. This improves over the standard method of guaranteeing coverage which requires pre-placing of tracks in an overly conservative manner.

III. Preliminary Results

The system is tested using a combination of open source tools, including incremental smoothing and mapping (iSAM) [16] for graph optimization, mission-oriented operating system with interval programming (MOOS-IvP) [17] for visualization and vehicle simulation and control, lightweight communications and marshaling (LCM) [18] for message passing and 3-D visualization, and Goby [19] for acoustic message encoding and decoding.

A snapshot of the system is shown in Fig. 8. In this case two vehicles are simulated, with both estimated position and

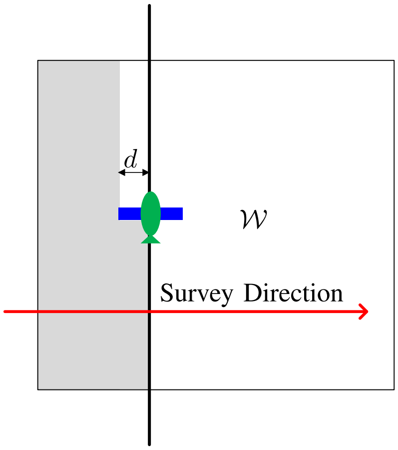

Fig. 7. The optimal value of d is calculated such that the vehicle achieves maximal coverage while still guaranteeing full coverage in the survey direction. A feedback controller is used to update the transect location in real-time to track the desired value of d.

ground truth position shown for each vehicle. The coverage grids are shown for each vehicle using the same color scheme as above: more blue indicates less covered and more red indicates more covered. The decentralized pose graphs of the two vehicles are shown at the bottom of Fig. 8.

We have performed a preliminary analysis in simulation to compare the cooperative and non-cooperative cases and show the benefits of the proposed approach. The paths for the two cases for the mission shown in Fig. 8 are shown in Fig. 9 and the traces of the instantaneous position uncertainties (i.e. not the smoothed estimates) are shown in Fig. 10. Since the position uncertainty is lower, as shown in Fig. 10, the adaptive planner can make the tracks further apart resulting in one fewer transects being necessary to cover the entire area up to the pre-specified confidence level. The path lengths are shown in Table I, and as we can see there is a reduction of about 17% in the path lengths resulting from the proposed approach.

TABLE I
PATH LENGTHS

	Cooperative	Not Cooperative
AUV 1	1757m	2112m
AUV 2	1755m	2113m

REFERENCES

[1] G. Davies and E. Signell, "ESPRESSO scientific user guide," NATO Underwater Research Centre, NURC-SP-2006-003, 2006.

[2] L. Paull, S. Saeedi, M. Seto, and H. Li, "AUV navigation and localization: A review," *Oceanic Engineering, IEEE Journal of*, vol. 39, no. 1, pp. 131–149, Jan. 2014.

[3] M. Bosse, N. Nourani-Vatani, and J. Roberts, "Coverage algorithms for an under-actuated car-like vehicle in an uncertain environment," in *Robotics and Automation, 2007 IEEE International Conference on*, april 2007, pp. 698–703.

[4] T.-K. Lee, S.-H. Baek, Y.-H. Choi, and S.-Y. Oh, "Smooth coverage path planning and control of mobile robots based on high-resolution grid map representation," *Robotics and Autonomous Systems*, vol. 59, no. 10, pp. 801–812, 2011.

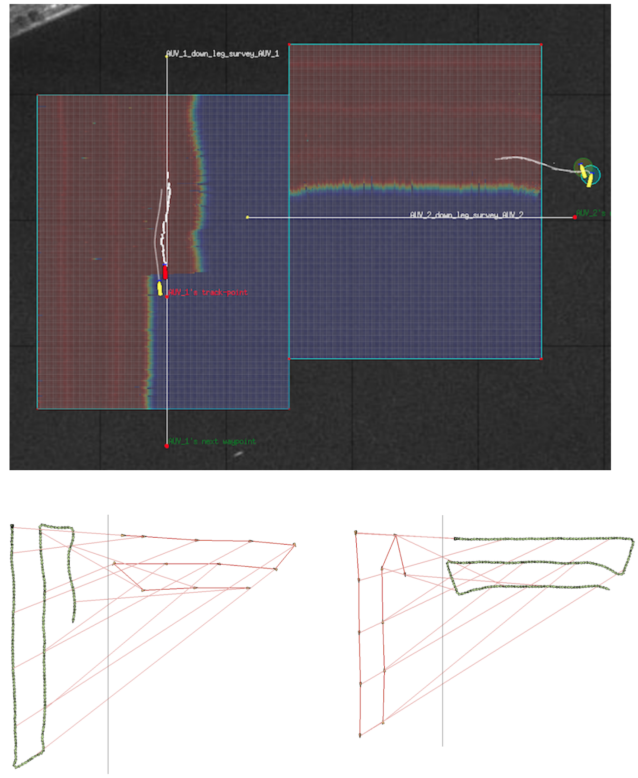

Fig. 8. A snapshot of the simulation in progress. *Top*: The two vehicles are underway in their respective areas. AUV 1 is performing north-south transects and moving towards the east. AUV 2 is performing east-west transects and moving south. The coverage maps are shown for each vehicle, where red areas are more covered and blue areas are less covered. At the time of the snapshot shown, AUV 2 is in the process of receiving an acoustic packet, as shown by the cyan circle around the vehicle on the right hand side. *Bottom*: The multi-vehicle pose graphs are shown (AUV 1 on left, AUV 2 on right). The dense green line is the own vehicle trajectory, and the sparse red line is the other vehicle poses at communication/measurement times. Own poses and other vehicle poses are connected through relative range constraints shown in pink.

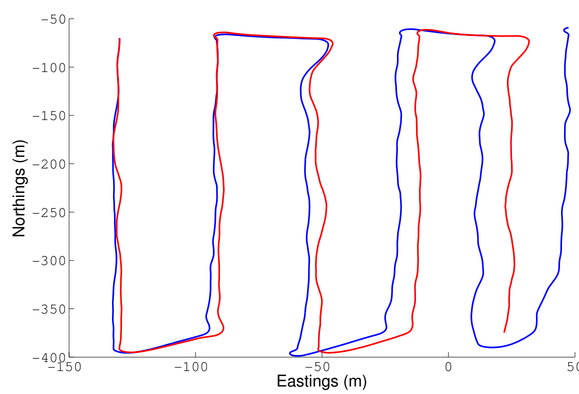

Fig. 9. The paths taken to cover the workspace by AUV 1 on the left hand side of Fig. 8 in the cooperative (red) and non-cooperative (blue) cases. In the cooperative case, the adaptive path planner is able to make paths more spaced out and consequently the vehicle is able to complete the mission with one fewer transects.

[5] C. Das, A. Becker, and T. Bretl, "Probably approximately correct cov-

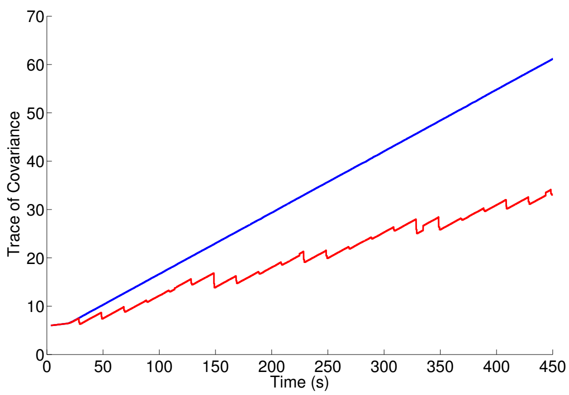

Fig. 10. The trace of the instantaneous covariances ($\sigma_{xx}^2 + \sigma_{yy}^2$) for the cooperative (red) and non-cooperative (blue) cases.

erage for robots with uncertainty," in *Intelligent Robots and Systems (IROS), 2011 IEEE/RSJ International Conference on*, sept. 2011, pp. 1160–1166.

[6] N. Trawny, S. Roumeliotis, and G. Giannakis, "Cooperative multi-robot localization under communication constraints," in *Robotics and Automation, 2009. ICRA '09. IEEE International Conference on*, May 2009, pp. 4394–4400.

[7] E. D. Nerurkar, K. X. Zhou, and S. Roumeliotis, "A hybrid estimation framework for cooperative localization under communication constraints," in *Intelligent Robots and Systems (IROS), 2011 IEEE/RSJ International Conference on*, 2011, pp. 502–509.

[8] E. Nerurkar and S. Roumeliotis, "A communication-bandwidth-aware hybrid estimation framework for multi-robot cooperative localization," in *Intelligent Robots and Systems, International Conference on*, Nov 2013, pp. 1418–1425.

[9] S. Webster, J. Walls, L. Whitcomb, and R. Eustice, "Decentralized extended information filter for single-beacon cooperative acoustic navigation: Theory and experiments," *Robotics, IEEE Transactions on*, vol. 29, no. 4, pp. 957–974, Aug 2013.

[10] A. Bahr, J. J. Leonard, and M. F. Fallon, "Cooperative localization for autonomous underwater vehicles," *The International Journal of Robotics Research*, vol. 28, no. 6, pp. 714–728, Jun. 2009.

[11] M. Fallon, G. Papadopoulos, and J. Leonard, "A measurement distribution framework for cooperative navigation using multiple AUVs," in *Robotics and Automation (ICRA), 2010 IEEE International Conference on*, May 2010, pp. 4256–4263.

[12] J. M. Walls and R. M. Eustice, "An exact decentralized cooperative navigation algorithm for acoustically networked underwater vehicles with robustness to faulty communication: Theory and experiment," in *Proceedings of the Robotics: Science & Systems Conference*, Berlin, Germany, June 2013.

[13] L. Paull, G. Huang, M. Seto, and J. J. Leonard, "Communication-constrained multi-AUV cooperative SLAM," in *IEEE International Conference on Robotics and Automation*, 2015, pp. 6592–6599.

[14] L. Paull, M. Seto, and H. Li, "Area coverage that accounts for pose uncertainty with an AUV surveying application," in *IEEE International Conference on Robotics and Automation*, 2014, pp. 6592–6599.

[15] L. Paull, M. Seto, and J. Leonard, "Decentralized cooperative trajectory estimation for autonomous underwater vehicles," in *Intelligent Robots and Systems (IROS 2014), 2014 IEEE/RSJ International Conference on*, Sept 2014, pp. 184–191.

[16] M. Kaess, A. Ranganathan, and F. Dellaert, "iSAM: Incremental smoothing and mapping," *Robotics, IEEE Transactions on*, vol. 24, no. 6, pp. 1365–1378, Dec. 2008.

[17] M. Benjamin, P. Newman, H. Schmidt, and J. Leonard, "An overview of MOOS-IvP and a brief users guide to the IvP Helm autonomy software," http:// dspace. mit. edu/ bitstream/ handle/ 1721.1/45569/ MIT-CSAIL-TR-2009-028.pdf, June 2009.

[18] A. Huang, E. Olson, and D. Moore, "LCM: Lightweight communications and marshalling," in *Intelligent Robots and Systems (IROS), 2010 IEEE/RSJ International Conference on*, Oct 2010, pp. 4057–4062.

[19] T. Schneider and H. Schmidt, "Model-based adaptive behavior framework for optimal acoustic communication and sensing by marine robots," *Oceanic Engineering, IEEE Journal of*, vol. 38, no. 3, pp. 522–533, July 2013.